Supplementary Information for

Additive-Specific Modulation of Non-Classical

Nucleation Pathways

Annet Baken,[*,†,‡] Alejandro Fernandez-Martinez,[‡] Martine Lanson,[‡] Xavier Mendez,[¶] Hegoi Manzano,[¶] Matthias Kellermeier,[§] Marco Di Michiel,[†] and Alexander E.S. Van Driessche[∥]

[†]ESRF

[‡]ISTerre, Univ. Grenoble-Alpes, CNRS

[¶]Euskal Herriko Unibertsitatea UPV/EHU

[§]BASF SE

[∥]IACT CSIC-UGR

E-mail: annet.baken@gmail.com

Contents

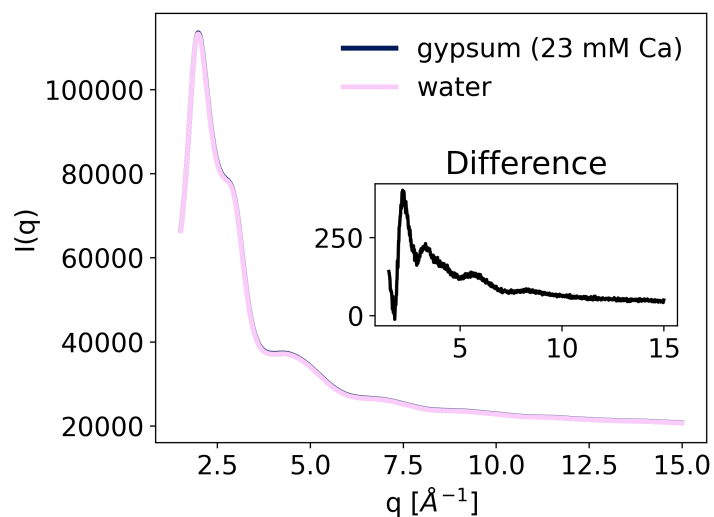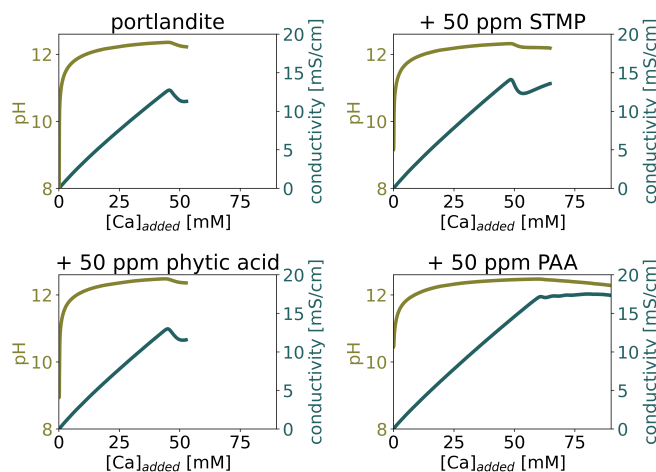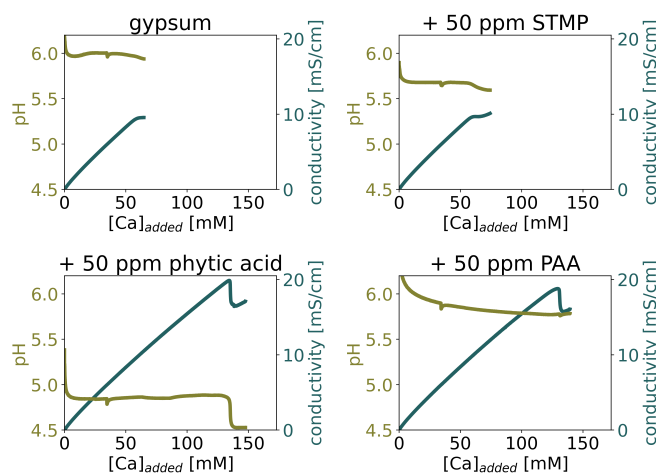# Supplementary Note 1: Difference between Background and Sample *I(q)*

Figure S1: $I(q)$ dataset of a gypsum precursor phase (23 mM added Ca) and $I(q)$ dataset of pure water. The inset shows the difference between the gypsum and water $I(q)$.

# Supplementary Note 2: Additional Co-titration Data

(a)

(b)

Figure S2: Conductivity and pH data of the nucleation of portlandite (a) and gypsum (b), in absence and presence of different types of additives. All curves represent the average of three repetitions, except for portlandite + PAA, gypsum + phytic acid and gypsum + PAA, as these experiments showed too much variance between repetitions.
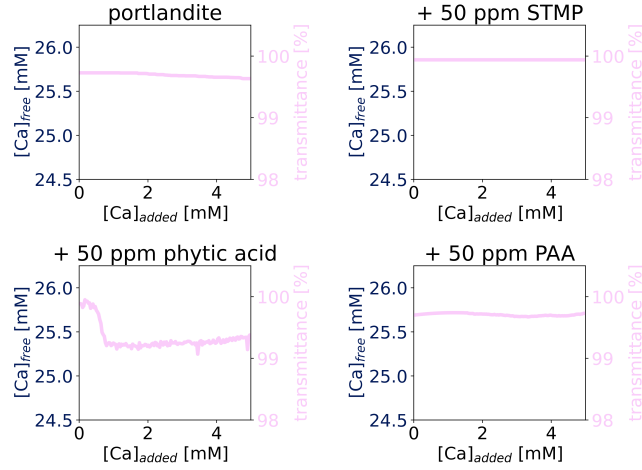
(a)
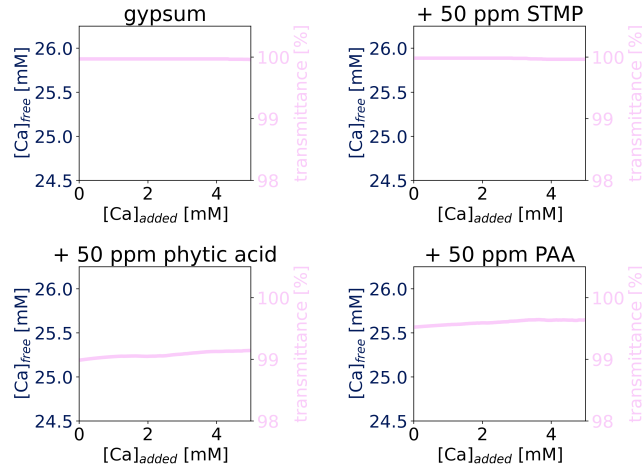
(b)

Figure S3: Detailed view of the transmittance data of the nucleation of (a) portlandite and (b) gypsum, in absence and presence of different types of additives. All curves represent the average of three repetitions, except for portlandite + PAA, gypsum + phytic acid and gypsum + PAA, as these experiments showed too much variance between repetitions.
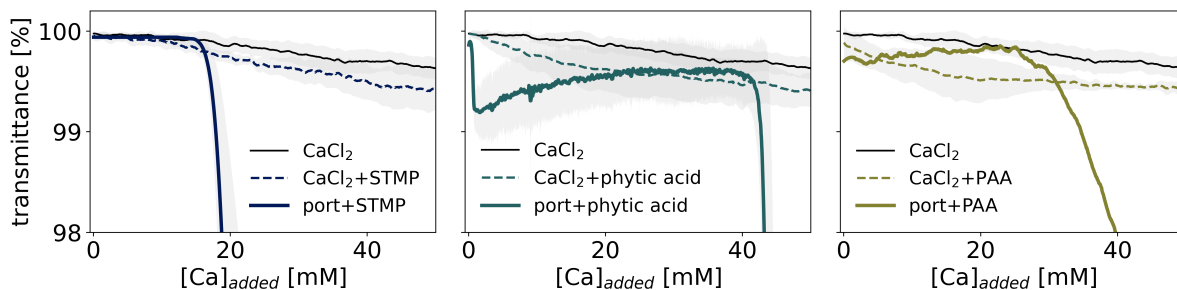
Figure S4: Transmittance data for a titration of 0.5 M CaCl$_2$ into 50 mL de-ionised water (black curve) and 50 mL de-ionised water containing 50 ppm STMP (dashed dark blue curve), 50 ppm phytic acid (dashed teal blue curve) or 50 ppm PAA (dashed green curve). The transmittance curves are compared with the data originating from the corresponding portlandite co-titration experiment. The plots are based on three measurements, of which the standard deviation is depicted in shaded grey.

Figure S5: Transmittance data for portlandite co-titration experiments in the presence of 500 ppm STMP (pink curve) or 500 ppm phytic acid (green curve).

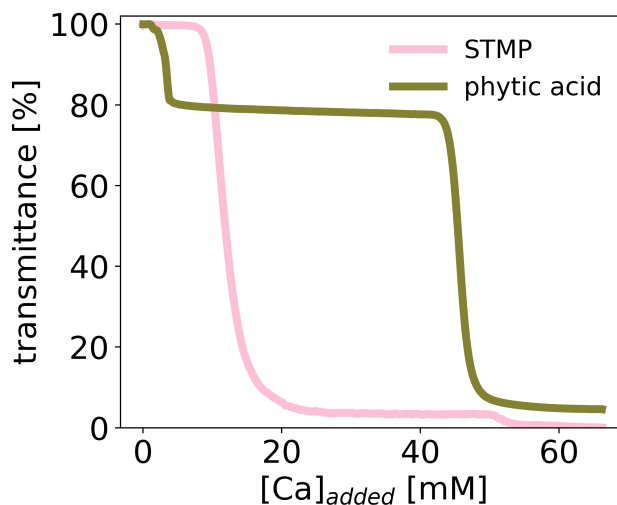# Supplementary Note 3: IR spectra
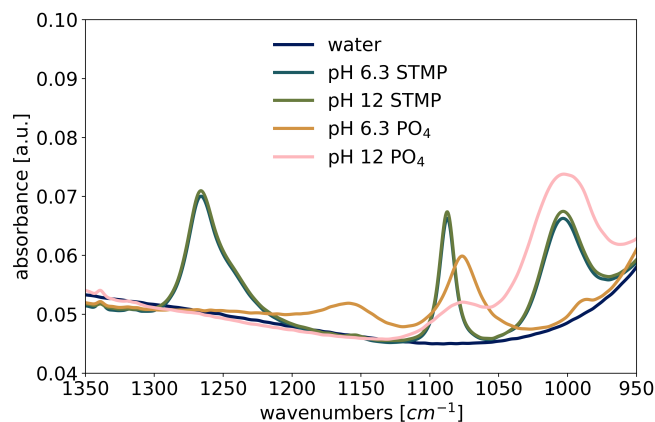
Figure S6: Infrared (IR) spectra obtained from solutions of STMP at pH 6.3 and pH 12, and solutions of potassium phosphate at pH 6.3 and pH 12. The pH was adjusted by adding KOH. The IR spectra were obtained with a Nicolet iS50 infra-red spectrometer of Thermo Scientific. A single-reflection diamond crystal was employed to analyze the solutions using the attenuated total reflection (ATR) method. For each sample, 32 spectra were averaged, with a spectral resolution of 4 cm^{-1}.

Supplementary Note 4: PHREEQC Calculation on Phytate Speciation

The PHREEQC calculation of the phytate speciation during the co-titrations directed to precipitate portlandite and gypsum, respectively, was based on complexation constants defined in Crea et al..[1] In addition to the complexation constants between phytate and calcium, this database contained the contants between phytate and sodium. As the anion-containing stock solution was NaOH for the portlandite systems and Na_2SO_4 for the gypsum systems, it was important to consider sodium-phytate complexation. Ultimately, at high pH levels (as in the portlandite system), the complexation between sodium and phytate was found to be stronger than the complexation between calcium and phytate (Figure S7).
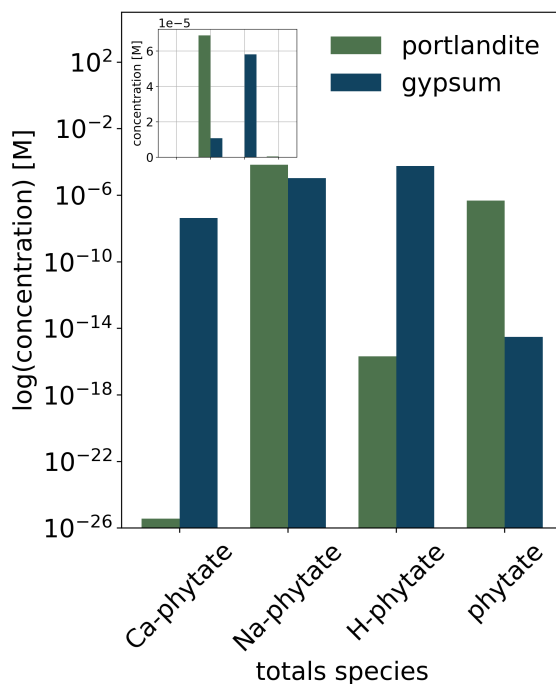

Figure S7: PHREEQC calculation of the total concentration (depicted on a log-scale) of phytate-containing complexes in the portlandite or gypsum system, at its solubility. The inset presents the same data on a linear scale. The complexation constants of phytate with calcium, sodium and hydrogen are obtained from Crea et al..[1]

Supplementary Note 5: Center of Mass and Variance Calculations

The nucleation pathway of portlandite and gypsum, both in the presence and absence of additives, was monitored at the nanoscale using *in situ* HEXS. Each HEXS measurement resulted in an intensity $I(q)$ curve, which was tracked over time or added calcium concentration. To quantify the general development of intensity, we calculated the center of mass from the $I(q)$ curve at increasing added calcium concentrations. Evaluating the center of mass position and variance of the scattering pattern at increasing added calcium concentrations provided insight into the evolution of the structure-related properties of the solution, as is depicted by two example scenarios in Figure S8.
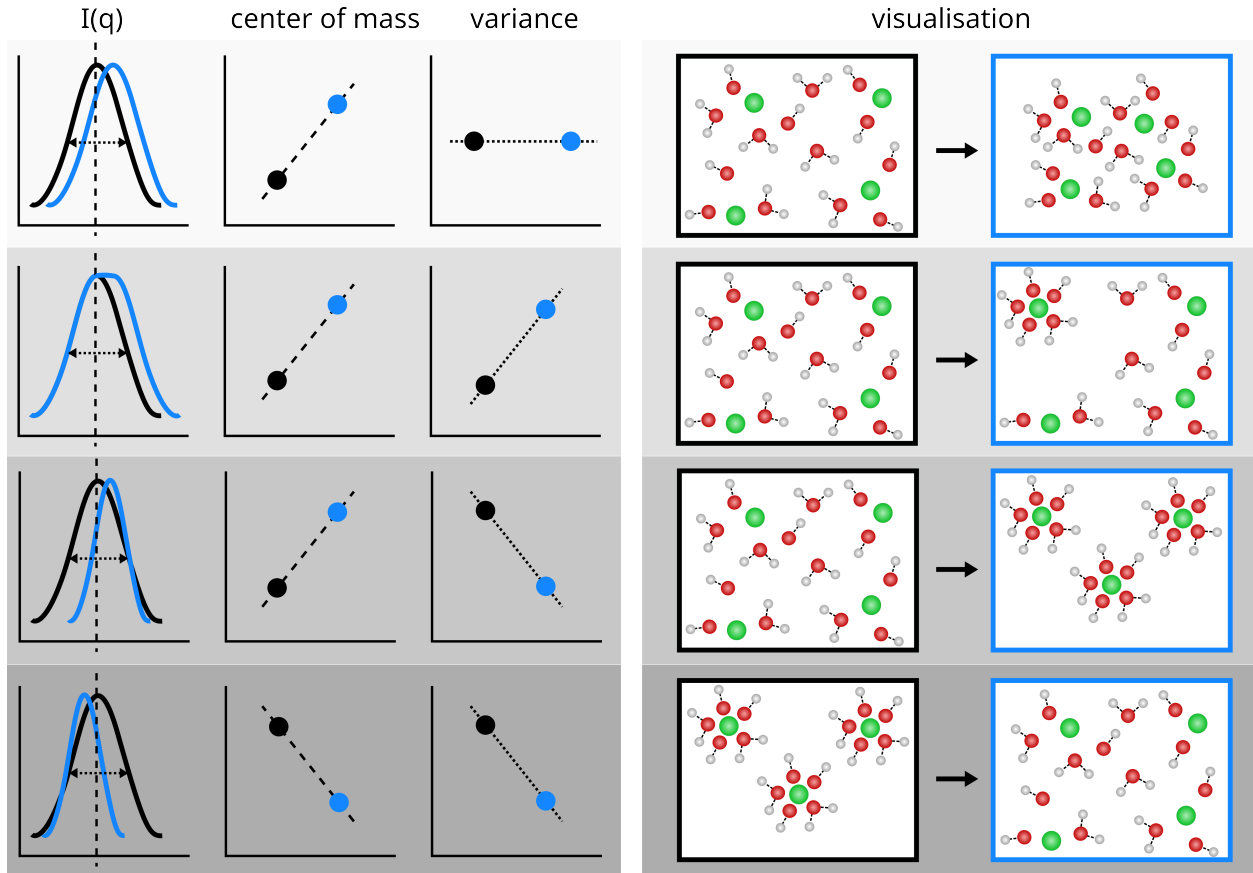
Figure S8: Explanatory figure for four different scenarios of the development of an $I(q)$ signal simplified to one peak. The different scenarios can be distinguished by analysing the change in the center of mass of the peak and the variance (related to peak width). Scenario (i): the peak displaces to higher q and does not change its shape, denoted by an increased center of mass and a stable variance. This can be visualised as the whole solution becoming denser. Scenario (ii): the peak widens due to the presence of an extra contribution at high q, denoted by a displacement of the center of mass to higher q and an increase in variance. This can be visualised as the appearance of a dense contribution denoted by the complex in the upper left of the image. Scenario (iii): the peak narrows but displaces to higher q, denoted by an increased center of mass and a decrease in variance. This can be visualised as the denser contributions dominating the sample, probably commencing to show some periodicity. Scenario (iv): the peak narrows and displaces to lower q, translating into a decrease in both the center of mass and variance. This can be associated with a reorganisation step.

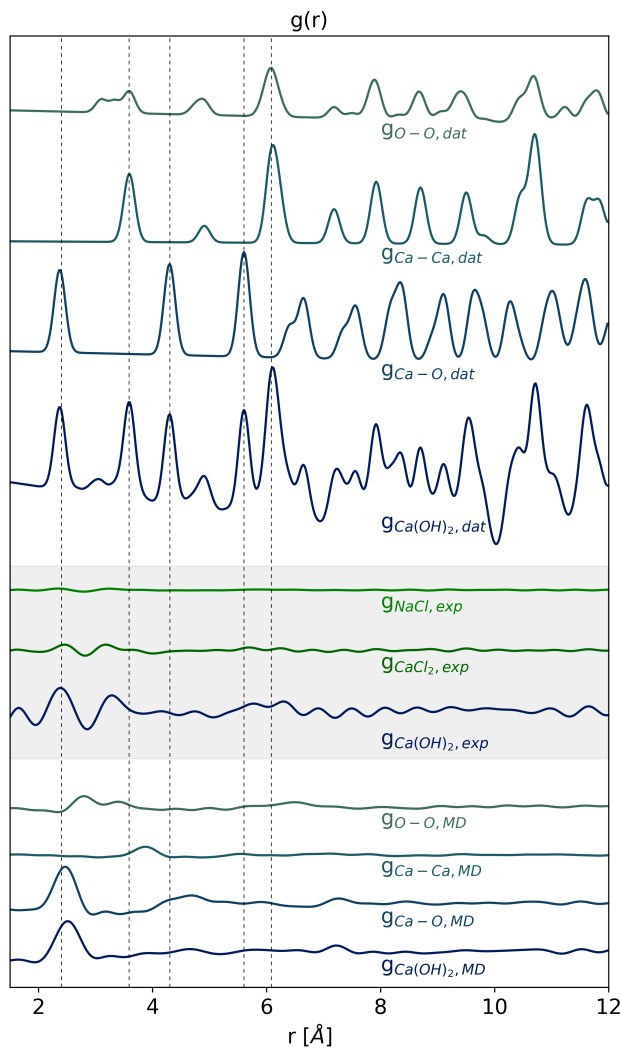# Supplementary Note 6: Molecular Dynamics Simulations

Figure S9: PDF patterns resulting from one of the last frames of an MD simulation of calcium, hydroxide and water at a density corresponding to the prenucleation stage of portlandite (MD). The patterns are depicted together with the PDF patterns of database (dat) portlandite[2] and the experimental PDFs (exp, grey background) of dissolved $CaCl_2$, NaCl and the prenucleation stage of portlandite.

Supplementary Note 7: Additional PDF Patterns
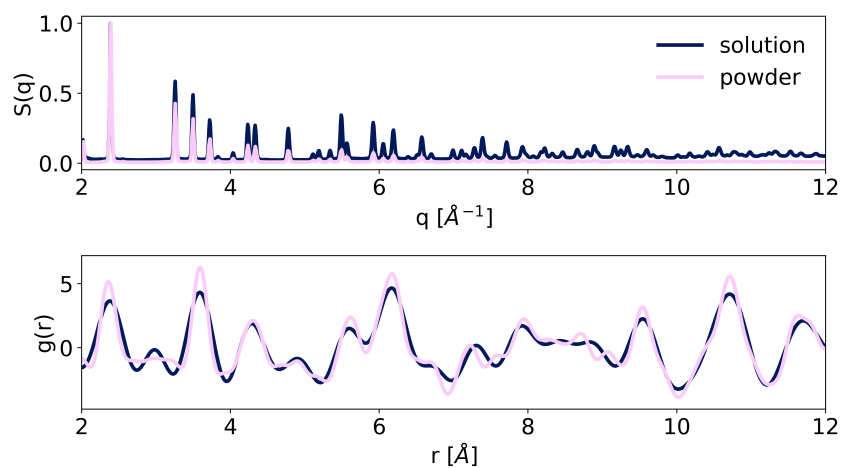
(a)
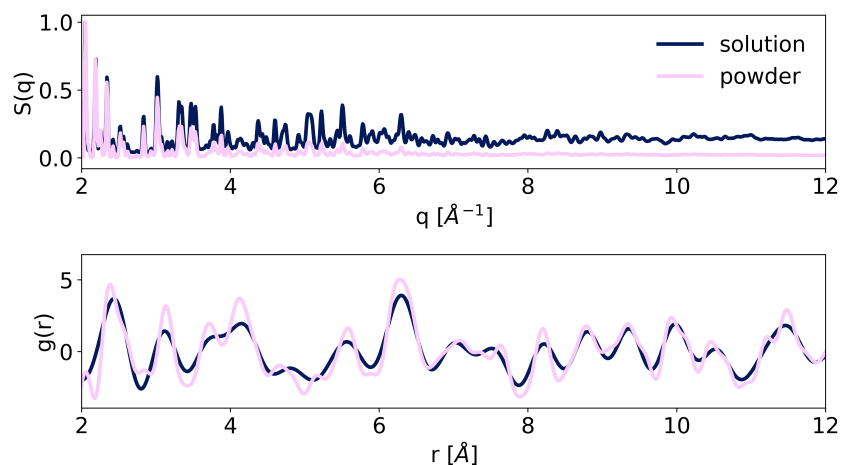
(b)

Figure S10: PDF and $S(q)$ patterns recorded from portlandite (a) and gypsum (b) containing solutions, compared to the patterns of crystalline portlandite and gypsum powders, respectively. The solutions were obtained from mixing $CaCl_2$ and $NaOH$ solutions (portlandite) or $CaCl_2$ and Na_2SO_4 solutions (gypsum) and were measured $\sim$ 6 hours after mixing.

Given the low statistics of individual scattering patterns obtained during the co-titration

experiments, scattering curves from the three characteristic stages were averaged to generate

PDFs, corresponding to the prenucleation stage, nucleation stage and crystallisation stage
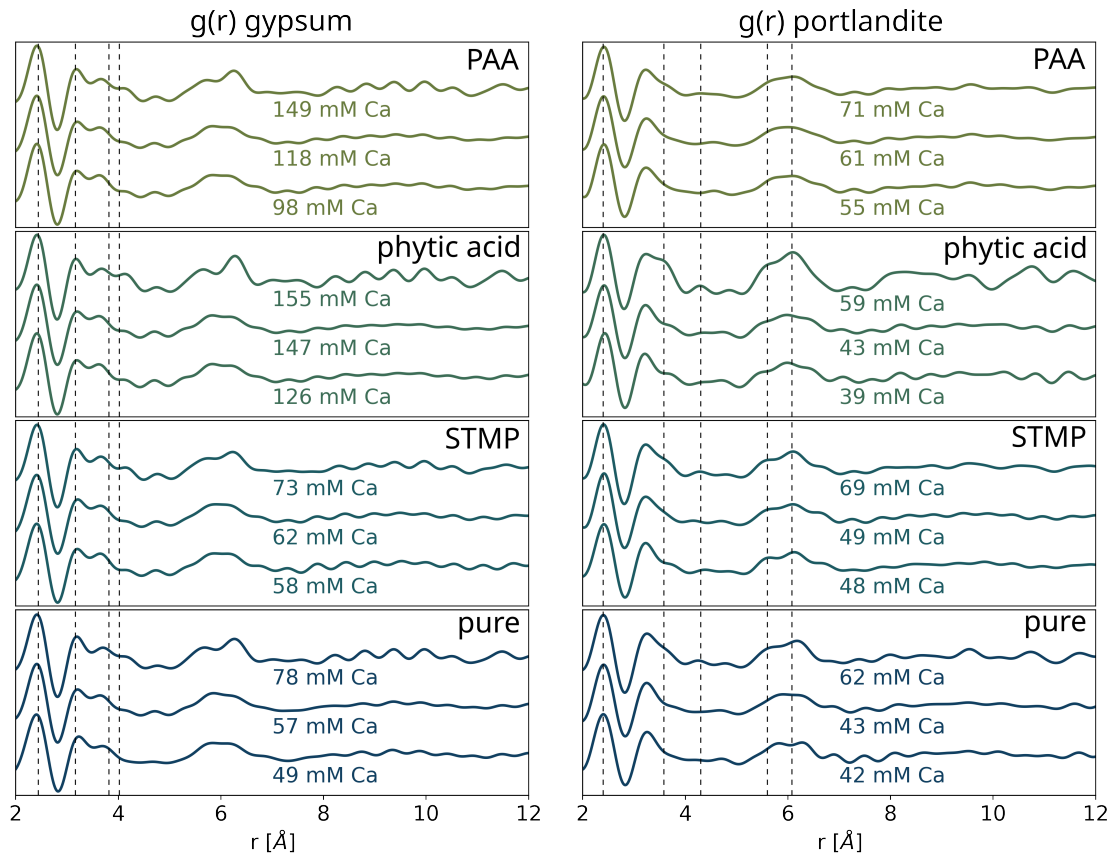
(in Figure S11).

Figure S11: PDF patterns of each portlandite and gypsum system, obtained at different time intervals/added calcium concentrations: prior to the decrease in free calcium concentration, between the decrease in calcium and the decrease in the transmittance, and subsequent to the transmittance decrease.

11

References

(1) Crea, P.; de Robertis, A.; de Stefano, C.; Sammartano, S. Speciation of phytate ion in aqueous solution. Sequestration of magnesium and calcium by phytate at different temperatures and ionic strengths, in NaCl. *Biophysical Chemistry* **2006**, *124*, 18–26.

(2) Busing, W. R.; Levy, H. A. Neutron Diffraction Study of Calcium Hydroxide. *The Journal of Chemical Physics* **1957**, *26*, 563–568.